

## Performance assessment of sustainable biocement mortar incorporated with bacteria-encapsulated cement-coated alginate beads

Prabhath Ranjan Kumar Soda <sup>a,1</sup>, Asheer Mogal <sup>a</sup>, Kalyan Chakravarthy <sup>a</sup>, Nikhil Thota <sup>a</sup>, Nimish Bandaru <sup>a</sup>, Sanjay Kumar Shukla <sup>b,2</sup>, K.M. Mini <sup>a,\*</sup>,<sup>3</sup>

<sup>a</sup> Department of Civil Engineering, Amrita School of Engineering, Coimbatore, Amrita Vishwa Vidyapeetham, India

<sup>b</sup> Founding Geotechnical and Geoenvironmental Engineering Research Group Leader, School of Engineering, Edith Cowan University, Joondalup, Perth, Australia



### ARTICLE INFO

**Keywords:**  
 Cement-coated alginate beads (CCAB)  
 Nano-silica  
*Bacillus megaterium* MTCC 8510  
 Microbially induced calcite precipitation  
 Compressive strength  
 Self healing

### ABSTRACT

Despite the extensive research on bacteria that are directly added to concrete to promote self-healing, studies on encapsulated bacteria have not been sufficient to comprehend crack healing. By employing *Bacillus megaterium* enclosed in cement-coated alginate beads, this research helps to improve the understanding of crack closure and the strength of self-healing mortar, which may be applied to the concrete. Autogenous healing occurs naturally, which will only repair micro-cracks. Moreover, it is a time-consuming process. Therefore, autonomous healing can assist in repairing little wider cracks with the addition of healing agents. *Bacillus megaterium* MTCC 8510 was used as the healing agent in the current study due to its ability to induce calcite precipitation (MICP) microbially. This was enclosed with alginate beads, and then coated with cement to form cement-coated alginate beads (CCAB). When a crack propagates, these beads break and generate  $\text{CaCO}_3$ , which clogs up the crack domain. Several tests, including compressive strength, water permeability, FESEM, surface healing and ultrasonic pulse velocity (UPV), have been carried out to understand the healing performance and other characteristics thoroughly. To determine the optimal amount of CCAB, these hardened cement-coated beads were mixed in mortar in different percentages of 10%, 15%, 20%, and 25% as a replacement for fine aggregate (FA). The reduced compressive strength, anticipated due to the addition of fragile beads, was compensated by adding nano-silica (NS) to maintain the minimum strength. The calcite precipitation was collected from the healed specimen and was observed under FESEM to analyse its microstructure. For 25% aggregate replacement, a healing percentage of 92.64% was attained in the internal domain of the crack with water permeability test, whereas 93.96% of the crack core was filled when checked using the UPV test each after 56 days. Specimens with 20% CCAB and 5% NS also satisfied the minimum criteria mentioned. Therefore, it is concluded that 20% sand replacement with CCAB containing 5% nano-silica is optimal for both strength and healing.

### 1. Introduction

Concrete is one of the most widely used building materials due to its low cost, durability and ease of usage in construction. Concrete has a high compressive strength, which aids in load bearing capacity. Over time, shrinkage, increase in permeability, environmental pollution, and other related factors lead to the deterioration of the strength and

durability of material [1]. Steel reinforcement bars are embedded in the structure to compensate for the tensile strength of concrete. Concrete becomes less durable and weakens the structure over a period of time due to shrinkage, increased permeability, environmental contamination and weathering. These factors contribute to the formation of micro-cracks on the surface of the concrete and within the structure. Disappointingly, micro-cracks increase permeability, allowing water and air

**Abbreviations:** PPC, Portland Pozzolana Cement; CCAB, Cement coated alginate beads; MICP, microbially induced calcite precipitation; UPV, ultrasonic pulse velocity; FA, fine aggregate; NS, nano silica; NB, nutrient broth; EC, electric conductivity.

\* Corresponding authors.

E-mail addresses: [s.shukla@ecu.edu.au](mailto:s.shukla@ecu.edu.au) (S.K. Shukla), [k\\_mini@cb.amrita.edu](mailto:k_mini@cb.amrita.edu) (K.M. Mini).

<sup>1</sup> ORCID: 0000-0002-9682-2708

<sup>2</sup> ORCID: 0000-0002-4685-5550

<sup>3</sup> ORCID: 0000-0002-5601-2209

<https://doi.org/10.1016/j.conbuildmat.2023.134198>

Received 22 July 2023; Received in revised form 10 November 2023; Accepted 13 November 2023

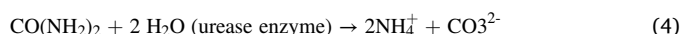
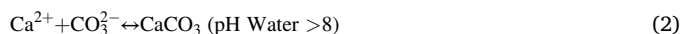
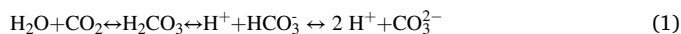
Available online 25 November 2023

0950-0618/© 2023 Elsevier Ltd. All rights reserved.

to penetrate the structure and corrode the embedded reinforcement bars. Because the reinforcement bars decay and the tensile strength of the cement concrete structure declines, microcracks negate the objective of placing reinforcement. They affect the structure's lifespan by reducing its durability.

It was reported that the cement and construction industry produced 8% of global CO<sub>2</sub> emissions (greenhouse gas emissions), making it the most polluting anthropogenic activity [2]. As a result, improving the service life of any infrastructure becomes a priority from both an economic and an environmental standpoint. An extended service life reduces the need for new infrastructure, lowering greenhouse gas emissions. Given this, the concepts of biocementation and self-healing concrete enter the picture for their potential application in improving infrastructure sustainability. The structure will regain strength by automatically activating the crack healing process. Small cracks automatically repair themselves in a specified environment during the self-healing process, whereas biocementation generally reduces the resilience of construction materials by increasing their strength.

Researchers are exploring various methods to heal the micro-cracks in concrete without affecting the performance of the structures. There are two types of healing processes: autogenous healing and autonomous healing [3]. The formation of CaCO<sub>3</sub> crystals due to the natural chemical processing without any external addition of healing agents is presented in the Eqs. (1) to (6) [4].



Various studies have suggested that autogenous self-healing occurs due to the formation of the C-S-H gel, the swelling of cementitious material in the crack domain, the formation of calcite, the covering up of fissures with tiny particles in the water, and the accumulation of tiny cracked pieces [5]. Autonomous healing occurs when an external healing agent is added to concrete or mortar. Adding healing agents can be done directly, through encapsulation, or through a vascular network system. The healing agents include fibres, minerals, microorganisms, shape memory alloys, polymers, etc. Direct addition of *Bacillus megaterium* cells to mortar can create vulnerable situations for the bacteria as it cannot withstand the mechanical and volumetric stresses during the mixing and hardening of concrete, respectively. The mechanical stresses caused by the impact of aggregates in the mixture during mixing may disturb the survival of bacteria. The pore sizes of the hardening mortar due to the formation of hydration products become lesser and lesser throughout the hydration process. Consequently, volumetric stresses developed on the cells in the pores can kill the vegetative cells. This environment cannot favour the more prolonged survival of bacteria. As a rectification, *Bacillus megaterium* has been encapsulated in beads which has an additional protection of cement coating. This setup can protect the bacteria from staying in the dormant stage for a longer life span and come into action when any sort of crack propagates via the beads in which bacteria are encapsulated. The fabrication process of this cement-coated alginate bead (CCAB) has been explained in Section 2.3.

The concept of self-healing concrete is one of the recent developments in the industry that has attracted a lot of attention, and it has the potential to be one of the most excellent solutions for cracks in concrete or mortar. It is reported that the addition of bacterial solution directly to conventional concrete raised the strength and longevity of the concrete [6]. However, spraying the bacteria on the surface of the cracks has been unsuccessful because it only treats the surface cracks and does

not treat the internal cracks. Another way is through the encapsulation technique, where the bacteria can be encapsulated into expanded perlite [7,8], diatomaceous earth [9], ceramsite [10], polyurethane, graphite nanoplatelets [11], ceramic pellets, silica gel [12], clay pellets [13], lightweight aggregate [14], polyurethane, cellulose fibre [1], sugar-coated expanded perlite [15], carbon black [16], nano carbon black [17], bio based fibre [33] etc. Several processes (such as natural, chemical, and biological) have been employed to design self-healing concrete. However, developing self-healing concrete using biological process has received significant attention among researchers. However, among the various encapsulation techniques, only a few works were reported on the successful sealing of embedded bacteria in alginate [18, 19]. The current study focused on the sealing performance of the coated beads along with the healing performance of the bacteria, strength, and durability of the mortar prepared by adding beads.

In the current work, the bacterial species chosen have a longer latent life period [20], high urease activity [21], and a reasonable amount of calcium precipitation. The nutrient broth was prepared and inoculated with *Bacillus megaterium*, and the beads were generated. *Bacillus megaterium* feeds on nutrient broth and survives inside the bead. Calcium required as a reactant for the chemical processing (Eqs. (5) and (6)) was added in the form of calcium chloride (CaCl<sub>2</sub>). When the bead breaks, the bacteria inside will assist in the formation of the urease enzyme. This urease enzyme catalyzes the reaction and eventually precipitates the calcite (CaCO<sub>3</sub>) as a product. The precipitated calcite acts as a healer in the crack domain. CCAB was used as a partial replacement for fine aggregates (FA) in various percentages, including 10%, 15%, 20%, and 25%. The compressive test was conducted to determine the appropriate percentage for replacement. The strength was naturally reduced because the CCAB is used instead of fine aggregate (FA). Nano-silica (NS) was added to the mortar in various percentages (1%, 2%, 5%, 8%, and 10%) as compensation for the strength of the specimen and to determine the appropriate percentage of NS to be added. The primary goals are to determine the optimal percentage of CCAB that must be replaced with FA and, the NS percentage that provides the greatest strength and healing performance.

## 2. Material and methods

### 2.1. Nutrient broth preparation

Nutrient broth (NB) is a medium in which *Bacillus megaterium* can survive and multiply in number. It was prepared by adding the constituents mentioned in Table 1. Each component in nutrient broth helps the growth of bacteria. Sodium chloride (NaCl) provides a source of electrolytes and helps to maintain osmotic balance, which is essential for bacterial growth. Peptone provides a balanced mix of amino acids, vitamins and minerals that are essential to promote the expansion of bacterial colonies, and its usage can result in more uniform and efficient bacterial growth. Yeast extract in nutrient broth provides a rich source of nitrogen, vitamins, and minerals that support the growth of bacteria. The extract acts as a fermentation substrate, promoting the production of ATP (Adenosine triphosphate) which is energy source at cellular level and other metabolites that are essential for bacterial survival and reproduction. Additionally, yeast extract can act as a buffer, maintaining a stable pH environment that suits the growth of most bacterial species.

**Table 1**  
Constituents of nutrient broth.

Constituent	Weight
NaCl	5 gm/l
Peptone	5 gm/l
Peptone-B	3 gm/l
Yeast extract	5 gm/l
Distilled water	1 l

A magnetic stirrer agitated and mixed the constituents uniformly without forming lumps. It was then transferred to conical flasks, each measuring 250 ml. These conical flasks were covered with paraffin tape and aluminium foil to avoid contamination. The nutrient broth is later autoclaved and sterilized for 15 min under a pressure of 15 kg/m<sup>2</sup> at 120° C. The sterilization process in an autoclave was done to remove undesirable microorganisms in the solution and dissolve the undissolved constituents in the nutrient broth [22]. After the sterilization process, the conical flasks were transferred to a basin filled with cool water to attain room temperature.

## 2.2. Culturing of *Bacillus megaterium*

*Bacillus megaterium* MTCC 8510 was obtained as a freeze-dried culture from the microbial type culture collection in Chandigarh, India. The selected bacteria are gram-positive and alkaliphilic. Due to these properties, the bacteria can survive and adapt to the highly alkaline environment inside the cement mortar. A cell wall with a thick outer cell is available in all gram-positive bacteria [23]. Thick cell wall protects the bacteria from sudden environmental change when mixed in concrete or mortar [24]. The growth condition of the bacteria is aerobic. The incubation time was set to 24 h at 37° C. Later, 5 ml of *Bacillus megaterium* solution was added to each flask, which was then covered with paraffin tape and aluminium foil on top to preserve it from the threat of contamination. The flasks were transferred to an orbital shaker to culture the bacteria. The temperature was set to 37° C, and the bacterial suspension was under shaking at 100 RPM for acceleration of growth. The bacteria was then subjected to heat shock treatment and sporulated. The spores are observed under fluorescence microscope as shown in Fig. 1. In this figure, the completely transformed vegetative cells into spores can be seen as the dots. By nature, *B. megaterium* as vegetative cell has rod shape and spores has a spherical shape. Hence it can be understood that after heat shock treatment, all the vegetative cells were converted to spores. The flasks were removed from the shaker after 24 h, and the cultured media appeared a little translucent and warm, signifying the presence of cultured *Bacillus megaterium*. The difference between nutrient broth with bacteria and pure nutrient broth without bacteria can be identified with the naked eye based on colour, opaqueness, and warmth.

## 2.3. Formation of bead

The cultured microbial solution was made into a gelatine solution by adding alginate powder, a substance inert to bacteria, and nutrient broth. Roughly no lumps were formed during the gradual addition of

alginate powder to the agitating bacterial solution. The properties of alginate are listed in Table 2. The solution was allowed to agitate for 25–30 min to form a lump-less gelatine solution with uniform viscosity. Eventually, after adding 20 g of alginate to 1 litre of bacterial solution, an alginate solution was formed, which had enough viscosity and was efficacious in forming proper spherical beads. The 20 g/l calcium chloride solution was prepared by using CaCl<sub>2</sub> and distilled water. The sucking and dripping off the gelatine alginate solution was done using a peristaltic dosing pump. A hypodermic needle of 0.3 mm was attached to the dosing pump's discharge pipe to allow smaller droplets to drip into the calcium chloride solution. After fixing the attachments, as shown in Fig. 2, the dosing pump was primed with water to ensure no air bubbles were formed in the beads. The suction pipe of the pump is dropped into the gelatine solution, which sucks the solution such that it falls in the form of drops at regular intervals on the discharging side. The calcium chloride solution was kept on a magnetic stirrer platform with turbulent swirling to prevent drops from collapsing on one another. The height between the surface of the beaker and the tip of the hypodermic needle was initially maintained between 15 cm and 25 cm. As the formation of beads takes place, slowly, the level of CaCl<sub>2</sub> solution raises. When a drop of gelatine alginate solution is dropped into a calcium chloride solution, a coating of Ca<sup>2+</sup> forms over the drop and forms a perfect spherical bead [25]. This process will be continued until the beaker runs out of alginate solution. After dropping the alginate solution into CaCl<sub>2</sub>, the magnetic stirrer was switched off, and the bead solution was filtered with filter paper as illustrated in Fig. 3. To ensure that the cement coating will adhere to the beads' periphery, they are then partially dried leaving some moisture all around them. The cement coating will shield the bead primarily against shrinkage and secondarily from internal moisture evaporation.

## 2.4. Cement coating over the beads

The prepared beads sustained its shape up to 7 days at 60% relative

**Table 2**  
Properties of alginate.

Property name	Description
Chemical name	(C <sub>6</sub> H <sub>8</sub> O <sub>6</sub> ) <sub>n</sub>
IUPAC name	Sodium;3,4,5,6-tetrahydroxyoxane-2-carboxylate
Colour	Cream Yellow
Odour	Mild
Texture	Fibrous
Solubility	Alcohol: Non-Soluble Non-Alcoholic: Gelatin Solution

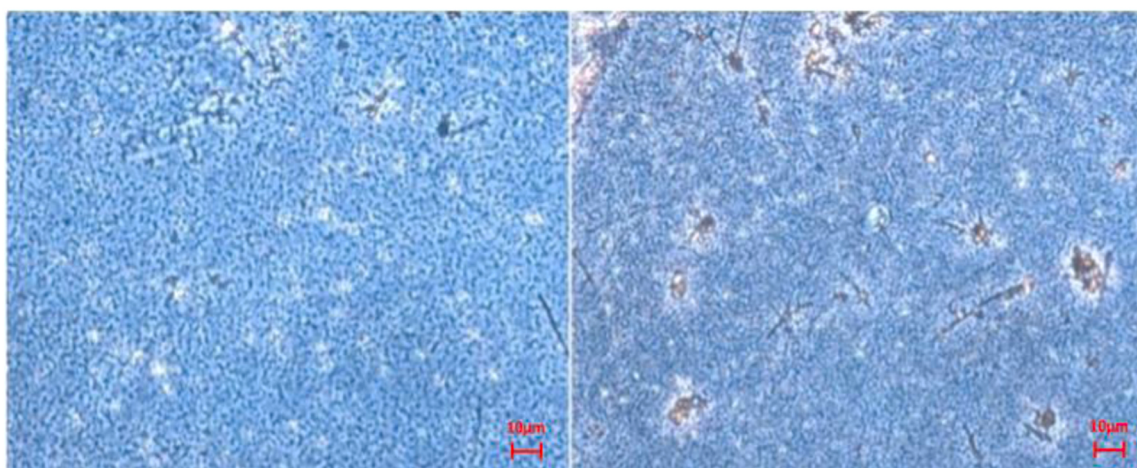


**Fig. 1.** Formation of spores from vegetative bacterial cells.

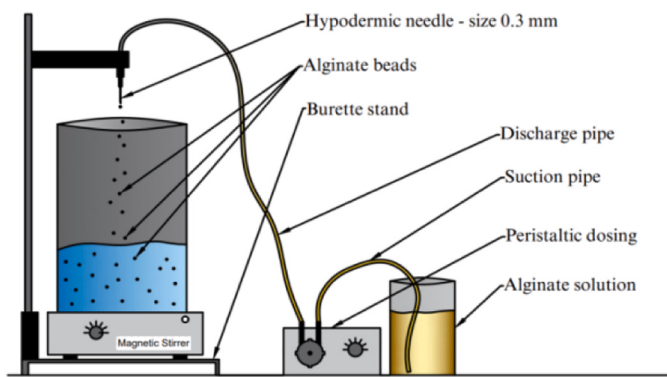


**Fig. 2.** Preparation of alginate beads.



**Fig. 3.** Alginate beads after filtration by filter paper.

humidity and at room temperature of 28 °C. But later, it was observed that the beads started shrinking by losing moisture and shriveled. These shriveled beads appeared to be stiff and rigid when tried to press between the fingers. This shows that the shriveled beads are useless as they do not rupture easily, and even though they rupture, urea hydrolysis will not begin. Hence experiments were conducted to address this issue by providing materials smeared over the beads. The sodium silicate and ordinary Portland cement (OPC) paste were considered to coat the beads initially. Since sodium silicate was water soluble and the coating may be disturbed during fresh mixing phases of mortar, OPC was not considered to coat with sodium silicate. Compared to OPC, Portland Pozzolana cement (PPC) was chosen because of its better durability and strength aspects and, the prolonged period of existence in the material. Finally, it was sussed out and discovered that a layer of Portland Pozzolana Cement (PPC) coating over the beads worked well. A trial-and-error procedure was utilized to establish the proper amount of cement to coat the beads. Based on the number of trials, the ratio of 1 kg of dry PPC to 1 kg of beads has arrived. Since the initial strength of the beads is less, hand mixing has been adopted by exerting light pressure on the mixture containing beads. Moreover, the cement coating can also increase the strength of the bead which will be favourable when mixing concrete or mortar.

After the coating, the beads were transferred to a mesh size of 2.36 mm sieve and agitated for 5 min on a sieve shaker to remove the excess cement. The produced beads were placed in an airtight container. After 24–48 hrs, the beads, which were stored in the air-tight container,

were ready for use. These beads were designated as Cement Coated Alginate Beads (CCAB). Fig. 4 shows the CCAB prepared, and Table 3 lists the parameters of the cement-coated alginate beads utilized in the study. A schematic representation of a layer of CCAB is shown in Fig. 5. The first layer is made of  $\text{Ca}^{+2}$  and alginate [25], while the periphery of the bead was coated with PPC. Cement coating keeps the beads away from shriveling and increases their strength. Gelatine alginate solution drops containing nutritional broth and *Bacillus megaterium* are present inside these layers, which participate in the chemical reaction once the crack propagation occurs.

## 2.5. Crack healing procedure

### 2.5.1. Preparation of cement mortar

Cement mortar with 1:3 proportion (1 part cement and three parts fine aggregate (FA) by weight) with a water-cement ratio (w/c) as mentioned in IS:4031 (Part 6)–1988 [26] was used in the study. Portland Pozzolana Cement (PPC) was used for the preparation of both bacterial and normal specimens. The cement has a standard consistency of 34 and a specific gravity of 2.9, and it complies with IS 12269–2013 [27]. Equal amounts of standard sand of grade I, grade II, and grade III with a specific gravity of 2.65 were utilized for the preparation. The fine aggregate requirements were in accordance with BIS 650:1991 (R2008). Fine aggregate is available in three grades: Grade I (1–2 mm), Grade II (0.5–1 mm), and Grade III (0.09–0.5 mm), and this grading is undertaken to ensure that the mix is well graded and will fill most of the voids in the mortar. In mixing water, urea (20 g/l) and calcium chloride (20 g/l) were used to mix the components of mortar and produce the necessary workability. Urea is a chemical reaction component, while calcium chloride is added as a part of the calcium source to form a calcite precipitate [28]. The nano-silica in varying percentages (1%, 2%, 5%, 8%, and 10%) by weight of cement was added to the mix to compensate for the alleviated strength of mortar due to the incorporation of cement-coated alginate beads in varying percentages (10%, 15%, 20%, and 25%) of fine aggregate. The manufacturing process of cement mortar samples for compressive strength testing conformed to IS: 4031-Part 6 [26]. In the control and bacterial specimens, a 1:3 mix proportion with varied water-cement ratios was used since the incremental addition of nano-silica necessitates more water. Furthermore, the control specimen was prepared using the same urea and  $\text{CaCl}_2$  solution but without including CCAB. The compressive strength and water permeability of the mortar sample were determined as per IS:4031 (Part 6)–1988[26] and IS:3085 (1965) [29]. All the specimens were subjected to 28 days of water curing at an ambient temperature.

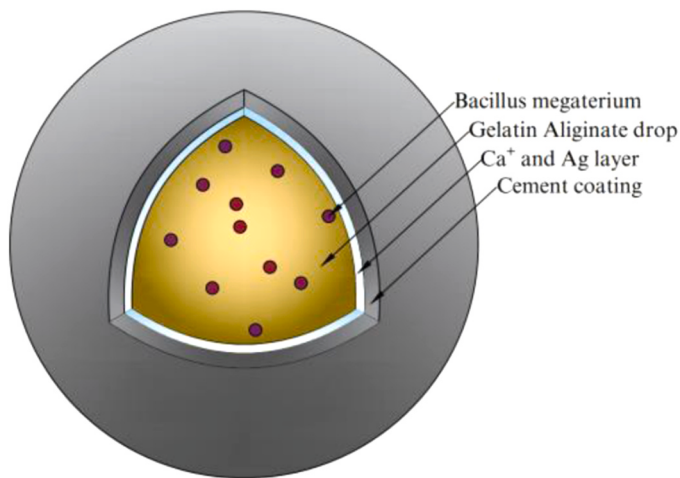


**Fig. 4.** Cement coated alginate beads (CCAB).

**Table 3**

Properties of beads.

Parameter	Property
Colour	Grey
Shape	Spherical
Diameter	2.4 mm
Coating type	PPC
Bacteria encapsulated	Bacillus Megaterium
Hardening time	24 hrs to 48 hrs.

**Fig. 5.** Illustration of inner view of CCAB.

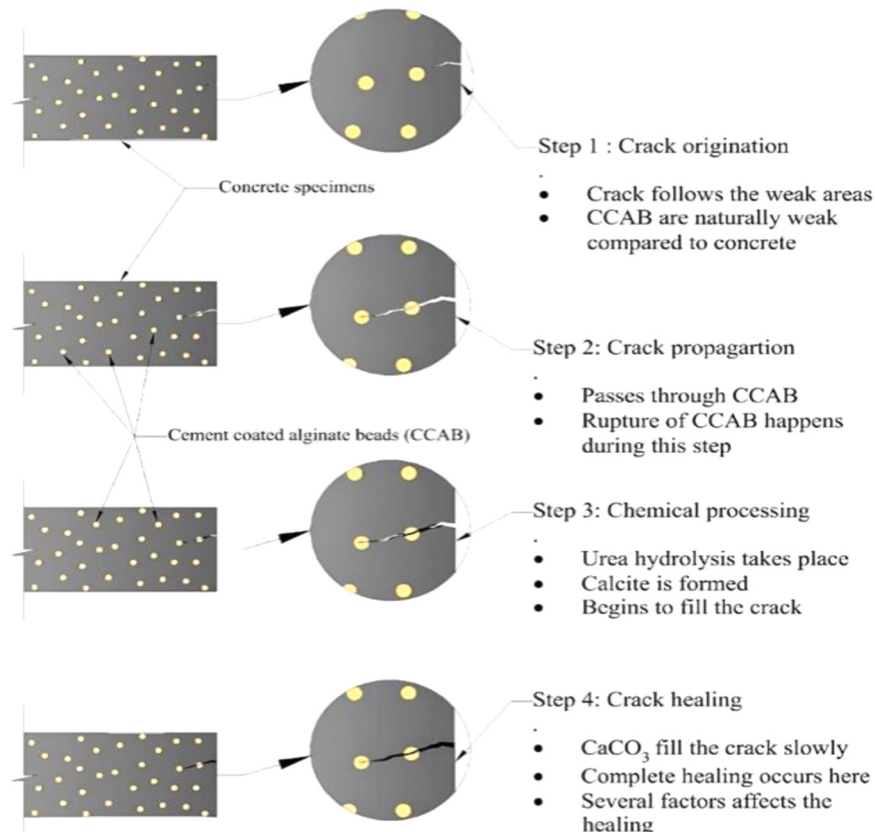
### 2.5.2. Healing mechanism

Due to the environmental conditions, concrete or mortar shrinks due to evaporation of the water in the concrete. Cracking happens when these shrinkage forces surpass the concrete's strength. The fracture seeks to expand via the weaker sections once it has been formed. To counteract this, CCAB was added to the mortar mix. These beads are inherently weak in comparison to the hardened mortar. Here, crack healing mechanism is shown schematically in Fig. 6. When a crack spreads, it will eventually pass through the beads (Step 1). Due to the fragility of the beads, they may rip off due to the mortar's rupture (Step 2), allowing Bacillus megaterium to react with the urea and calcium chloride added during the mortar preparation (Step 3). The further reaction with the carbonate ions produced by urea hydrolysis reacts with calcium ions leads to formation of calcite (Step 4) [30].

### 3. Experiments and formulation

#### 3.1. Compressive strength

The compressive strength of specimens was tested using UTM having loading capacity of 100 kN. The specimens were 70.6 mm × 70.6 mm × 70.6 mm cement mortar cubes treated in the water curing process. Three specimens of each varied combination of beads and nano-silica were tested for compressive strength, for a total of 72 specimens (excluding three control specimens). These findings were analysed, and the optimum solution was discovered. 200 g of PPC and 600 g of fine aggregate (FA) are needed to make a 1:3 cement mortar for a 70.6 mm cube. Every 600 g of FA contains three different grades of FA combined in equal proportions of 200 g each.

**Fig. 6.** Schematic representation of the healing mechanism in the specimen.

### 3.2. Water permeability test

Water permeability test determines the efficacy of bacterial healing in the concrete core crack. A test setup was made up for conducting the test. Before testing water permeability, cylindrical specimens of 20 mm thick and 100 mm in diameter were moulded and water cured for 28 days. Specimens with 10%, 15%, 20%, and 25% substitution of FA with CCAB were used. A crack was artificially developed by placing a steel bar as shown in Fig. 8, and by applying gradual load on the top of the specimen with the bar using a universal testing machine (UTM) at a regulated loading of 1.5 mm/min. Later, the cracked cement mortar specimen was sandwiched between a measuring jar and a porcelain funnel to make the water permeability testing instrument, as shown in Fig. 7. Cracked cement mortar specimen was attached with silicone sealant and then taped over the dry sealant as shown in Fig. 7. The time taken for 1 litre of water to flow entirely from the measuring jar to the collecting jar is recorded on the 0th, 3rd, 7th, 14th, 21st, and 28th days. The same cement mortar mix proportion of 1:3 was used to examine the water permeability. Three specimens of each kind were used to evaluate the average permeability.

Eq. (7) was used to evaluate the coefficient of water permeability.

$$C_w = \frac{1000}{w \times l \times t} \quad (7)$$

where  $C_w$  is the coefficient of water permeability,  $w$  is the average width of the crack,  $l$  is the length of the crack, and  $t$  is the time taken for 1 litre of water to flow through the crack.

### 3.3. Analysis of cracked surface

The crack domain gradually fills up with calcite precipitated by *Bacillus megaterium*. Measuring the surface area of the fracture domain on the first day of restoration and after a significant number of days can disclose the days it takes to heal a specific quantity of surface area. The percentage of the surface area restored with precipitation after 3 days, 7 days, 14 days, 21 days, and 28 days was calculated using Image J software. The specimens for this test are cubical and 50 mm in size. By applying an external load perpendicular to the surface across which the crack is required, a fracture was artificially produced on the 50 mm cube using UTM. Once the surface cracks are formed in the specimens, they are monitored by photographing the crack, using a macro lens, after 3, 7, 14, 21, and 28 days for each specimen. Eq. (8) was used to compute the percentage of the surface area healed.

$$R = \frac{A_i - A_o}{A_o} \times 100 \quad (8)$$

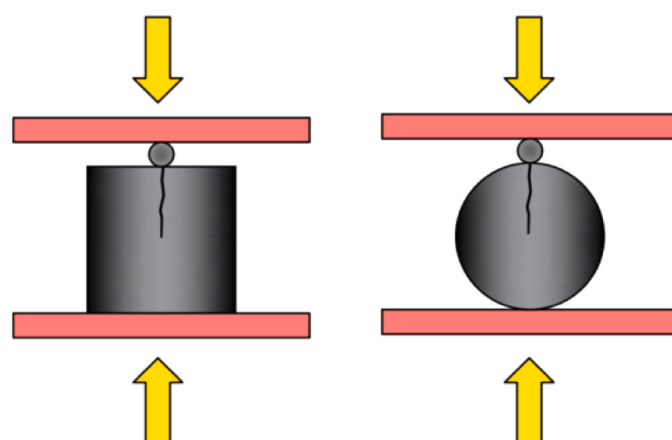


Fig. 8. Formation of artificial crack.

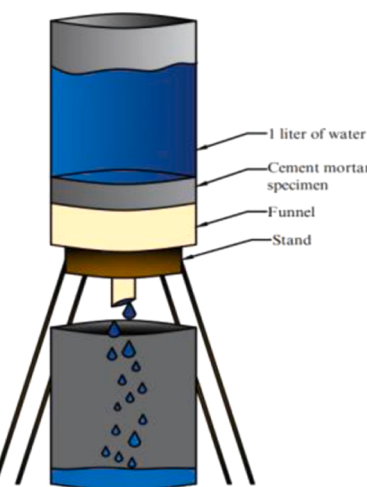


Fig. 7. Water permeability test apparatus.

where  $R$  represents the rate of crack area repair in percentage,  $A_o$  is the unhealed crack area, and  $A_i$  is the healed crack area at the time of  $i$ . Once the calibration was done, using the segmented line tool, the crack area was traced precisely, and then the average width and area of the cracks were found. The average width was estimated by measuring the width of the crack at 5 different places, as shown in Fig. 9(a, b, c, d) for 10%, 15%, 20%, and 25% replacement specimens. The average of these numbers represents the width of each crack.

### 3.4. Ultrasonic pulse velocity test (UPV)

The internal percentage healing of the crack domain portion was indirectly measured using the UPV test. This test is conducted by passing a pulse ultrasonic through mortar to be tested and measuring the time taken by the pulse to get through the structure. Higher velocities indicate good quality and continuity of the material, while lower velocities indicate concrete with many cracks or voids. Ultrasonic testing equipment includes a pulse generation circuit, consisting of an electronic circuit for generating pulses and a transducer for transforming an electronic pulse into a mechanical pulse having an oscillation frequency in the range of 40–50 kHz, and a pulse reception circuit that receives the signal (Fig. 10). Specimens chosen for this test are cubes of size 50 mm with 1:3 cement mortar mix that were cracked carefully. The healing of cracks by calcite precipitation accounts for the increase in velocity. The percentage increase in velocity indirectly indicates how well the cracked sample is healed. The percentage of healing cracks,  $H_p$ , was calculated by using Eq. (9).

$$H_p = \left( \frac{V_i - V_0}{V_0} \right) \times 100 \quad (9)$$

where  $V_i$  is the UPV measured on  $n^{\text{th}}$  day of healing and  $V_0$  is the UPV measured on 0th day of healing.

### 3.5. Efficiency of cement coating

Electric conductivity (EC) testing was used to determine the effectiveness of the cement coating. The mechanism of microbially induced calcite precipitation (MICP) via a ureolytic path boosts the calcite precipitation as a result of the ureolytic bacteria's activity of the urease enzyme. *Bacillus megaterium* is a ureolytic bacteria. Ammonia and carbonate ions are generated during the precipitation of calcium carbonate as a by-product of urea hydrolysis in the presence of urease enzyme, which is triggered by *Bacillus megaterium*, boosting the conductivity of the solution. A 1.11 M urea solution was made, and the electric conductivity of both broken and unbroken cement-coated beads

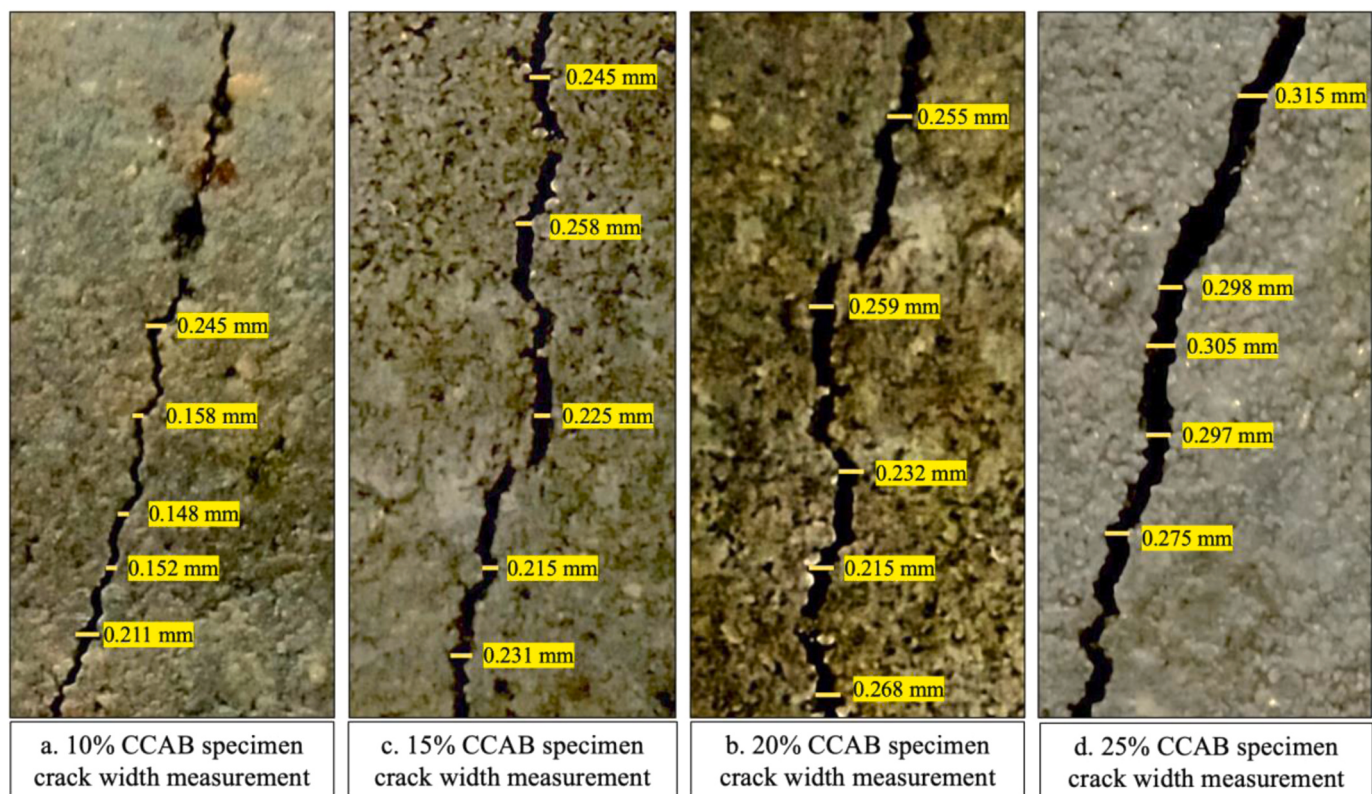


**Fig. 9.** Crack width measurement of various specimens.

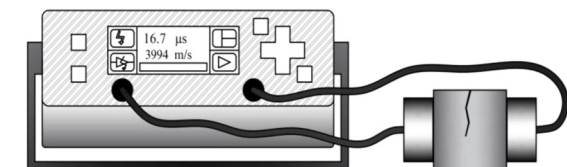


**Fig. 10.** UPV Analysis of a cube specimen.

was measured. In the 1.11 M urea solution, broken and unbroken beads were separately added. The electric conductivity of those samples was measured using a universal water quality analyzer at 5-minute intervals for 60 min. When compared to unbroken beads, the conductivity of fractured beads was observed to increase. From the test results, it was observed that the intact cement-coated beads have high coating efficiency. The coated beads were cured in a sealed container at room temperature for 3 days. The breaking load of the coated bead was determined using a S-type load cell having a capacity of 200 N with least count of 0.01 N. The test was conducted at a 0.001 mm/s rate of loading on 6 coated beads. The average breaking load was observed to be 7.2 N. The stresses that can occur in the mixing process of concrete due to coarse aggregate particles could be higher than the breaking load of the bead. Hence the application of coated alginate beads can be restricted to applications like plastering or similar kind of masonry works.

### 3.6. Regression analysis

A statistical software called the Minitab has been used to analyse the experimental results. By taking percentage aggregate replacement and nano silica percentage as the dependent variables, and compressive strength and percentage healing as independent variables based on the findings required, multiple regression analysis was used. These equations can assist in finding the magnitude of resultant parameters at

intermediate positions.

## 4. Results and discussion

### 4.1. Analysis of compressive strength

The compression test was done on three control specimens with a cement: sand ratio of 1:3, and the average compressive strength was found to be 23.62 N/mm<sup>2</sup>. The minimum compressive strength for a 1:3 cement mortar cube at 28 days, according to IS 2250–1981, should be 7.5 MPa, and all three control specimens met the requirement. Then 12 more mortar specimens were cast with a cement: mortar ratio of 1:3 and aggregate replacement in different proportions by weight (10%, 15%, 20%, and 25%) with CCAB. At 28 days, the cubes' compressive strength was measured.

It was also noticed that as more aggregates were replaced with beads, the more compressive strength dwindled. To compensate for the lost compressive strength due to the replacement of fine aggregate, nano silica was added to the mortar mix in different proportions of 1%, 2%, 5%, 8%, and 10% by weight of cement. The results of the compressive test are presented in Fig. 11. All the mortar specimens showed an increase in compressive strength after adding nano silica to the mix. There has been an increment in compressive strength up to 5% addition of nano silica, while further expansion resulted in a drop. The decrease in compressive strength could be due to the agglomeration of nano silica particles, which could have adversely affected the material's hydration and bonding strength [31]. The highest compressive strength was recorded as 19.99 MPa in the case of 10% FA replacement with 5% NS addition. The second highest was 15.82 MPa in the case of 15% FA replacement and 5% NS. 20% FA replacement with 5% NS specimens' compressive strength was 11.64 MPa. The compressive strength of 25% FA replacement with 5% NS addition was 7.47 MPa. As per IS 2250–1981, the minimum compressive strength of a 1:3 mortar specimen must be greater than or equal to 7.5 MPa. 25% CCAB with 5% NS

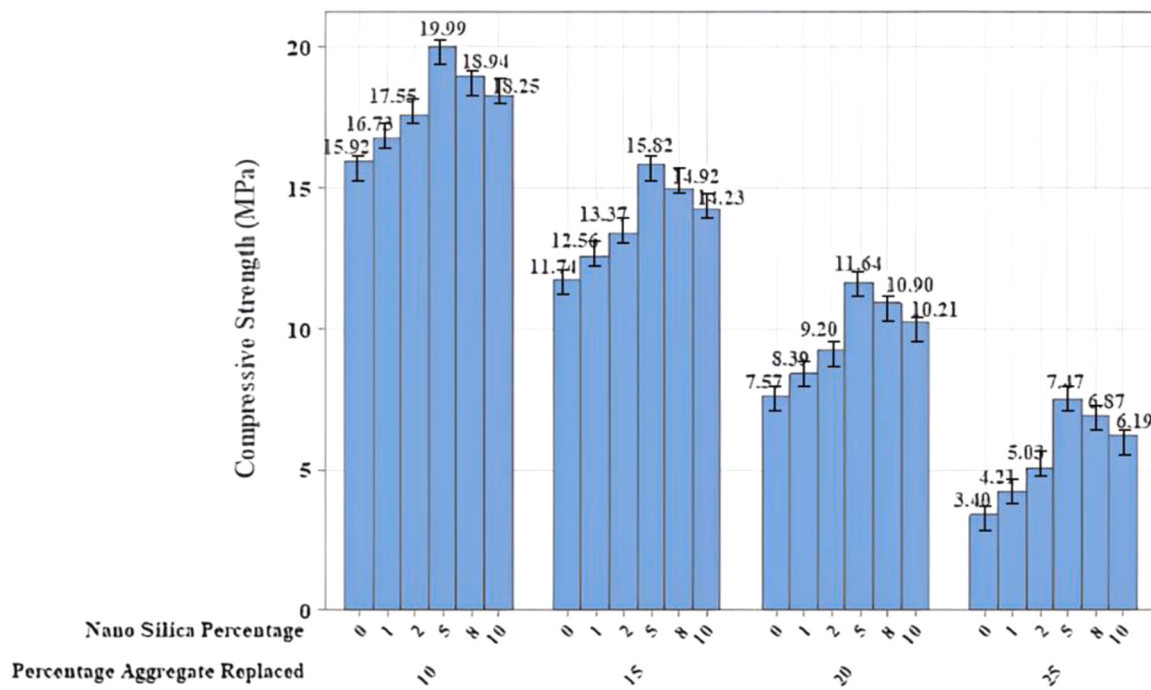


Fig. 11. Variation in compressive strength.

specimen slightly failed in achieving the minimum compressive strength. As a result, replacing FA with 25% of CCAB with any proportion of NS must not be used in any circumstances.

#### 4.2. Crack core healing analysis – water permeability results

The effect of FA replacement on healing in interior areas of concrete was also explored using a water permeability test, with aggregate percentages ranging from 10%, 15%, 20%, and 25% and healing percentages recorded on days 3, 7, 14, 21, 28 and 56 days respectively. Eq. (7)

was used to calculate the coefficient of water permeability ( $C_w$ ), and then the percentage of healing was calculated. Fig. 12 depicts the effect of percentage aggregate replacement on concrete healing at the innermost parts. For 25% aggregate replacement, as per Fig. 12, the maximum healing percentage (92.64%) was attained in the interior areas of the mortar. Also, increased crack healing is observed with more number of days. The reason behind the maximum healing at 56 days compared to 28 days might be because of the lower rate of formation of calcite inside the crack due to the less availability of oxygen. So, even though higher percentage of replacement leads to more availability of bacteria cells at

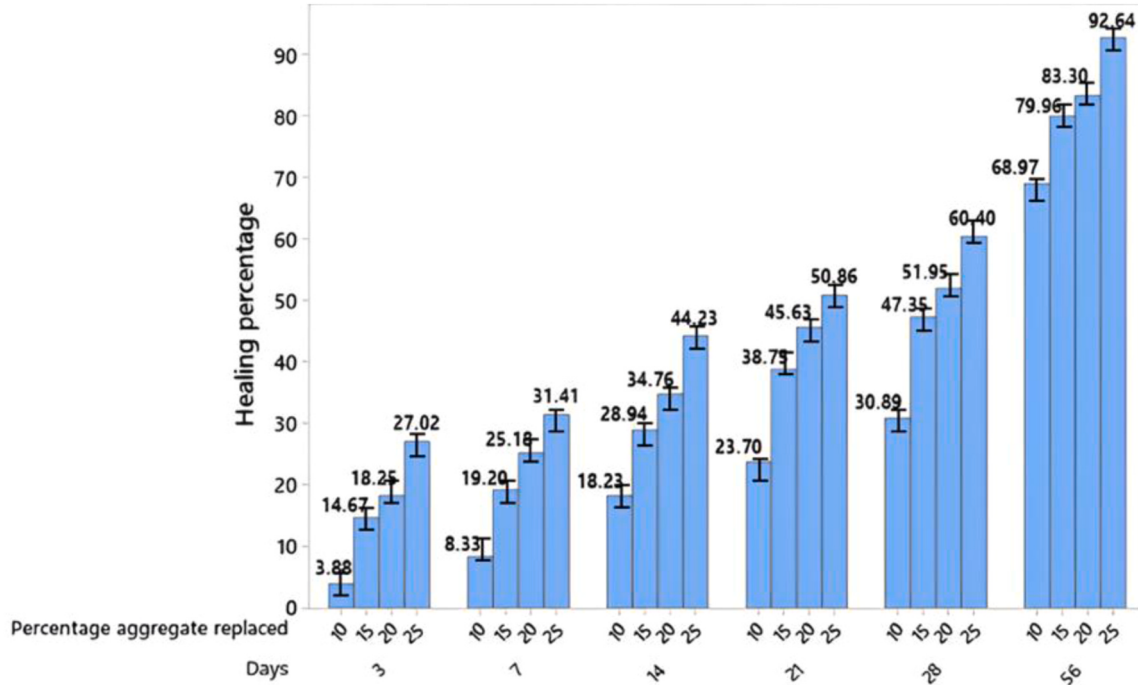


Fig. 12. Percentage healing of crack using water permeability test.

cracked location, delayed healing occurs due to the difficulty in availability of oxygen in the inner portion of crack.

#### 4.3. Crack core healing analysis - UPV results

The collected results were manually analysed by checking the percentage change in the adjacent values. There were 12 specimens, each of 3 in each different CCAB replacement. The average width of the crack was measured using Image J software, as mentioned in the surface healing test. The average width of the crack of all the specimens varied between 0.15 mm and 0.3 mm. After a visual examination of the magnitudes of percentage healing of the specimens on certain days (0th, 3rd, 7th, 14th, 21st, 28<sup>th</sup>, and 56th), it was understood that various factors might influence the amount of crack healing. Pulse velocities were noted for the uncracked specimens as well as for cracked specimens. These values were converted to a percentage by using Eq. (9). The values of the samples were averaged and presented in Fig. 13. The graph shows that 25% replacement with CCAB produces superior results because healing starts sooner than the other percentages. A 25% CCAB specimen had an average healing rate of 16.03% on the third day, which was more significant than all different percentages. It recovered more quickly and to a greater extent, which can stop the crack from spreading further. Because 25% replacement has the highest percentage of crack healing across all days and has healed 93.96% of the crack domain on day 56, it has been determined to be the best replacement for healing cracks. So the observation of healing at 56 days is similar to that of water permeability results. Both the tests are representing lesser healing percentages at 28 days compared to 56 days, which may be due to less availability of oxygen and moisture inside the crack.

#### 4.4. Crack width and surface healing

Fig. 14 presents the healing of the cracks in selected portions after 28 days. The surface crack domain has healed more than expected due to the abundant oxygen available near the surface. However, this does not ensure that the internal crack is also healed. Internal cracks may take longer time to heal, considering the parameters influencing the healing,

like width of the crack, the open/broken bacterial sources (CCAB in this study) along the undulated crack plane, the percentage of the bacterial source added in any form, the availability of moisture and the availability of oxygen (if the bacteria are aerobic) and the number of bacterial cells.

Maximum healing was observed in the 25% replacement due to more CCAB (Figure 14). Some intermediate areas of the cracks have not healed adequately, as shown in Fig. 14 corresponding to 10% and 20% replacements. This may be due to the lack of broken beads or since the healing has been observed only for 28 days. In Fig. 14, corresponding to 15% illustrates how the dried and shrunk bead formed a void with an average diameter of 2.4 mm, which was visually inspected and measured using image J software. As far as modern advancement is concerned, 2.4 mm width cannot be cured autonomously. According to data from additional research articles, the largest crack that healed was 0.97 mm wide [23]. Here, the average crack widths were extremely small, ranging from 0.1 to 0.25 mm, as seen in Table 4. The maximum crack width that can be repaired may also depend on the healing technique, in this example, encapsulation.

#### 4.5. Electric conductivity results

Fig. 15 shows the electric conductivity (EC) variations in micro siemens (ms) measured for 60 min with a class interval of 5 among three series. Series 1 represents the EC of CCAB with *Bacillus megaterium* (broken), series 2 represents the EC of CCAB only with alginate but no *Bacillus megaterium* (broken), and series 3 represents the EC of CCAB with *Bacillus megaterium* (unbroken). Series 2 and 3 do not have much variation in the electric conductivity and have an increment from 59  $\mu$ S to 66.56  $\mu$ S and 48.94  $\mu$ S to 59.12  $\mu$ S, respectively. Whereas series 1 began at 80.63  $\mu$ S and steadily increased to 180  $\mu$ S at the 60th minute. This means that the *Bacillus megaterium* has shown its action by breaking down the urea hydrolysis to ionize carbonate and ammonia. Due to this ionization, electric conductivity has increased in broken CCAB containing *Bacillus megaterium*. Even though the CCAB is broken in series 2, ionization has not occurred due to the absence of *Bacillus megaterium*.

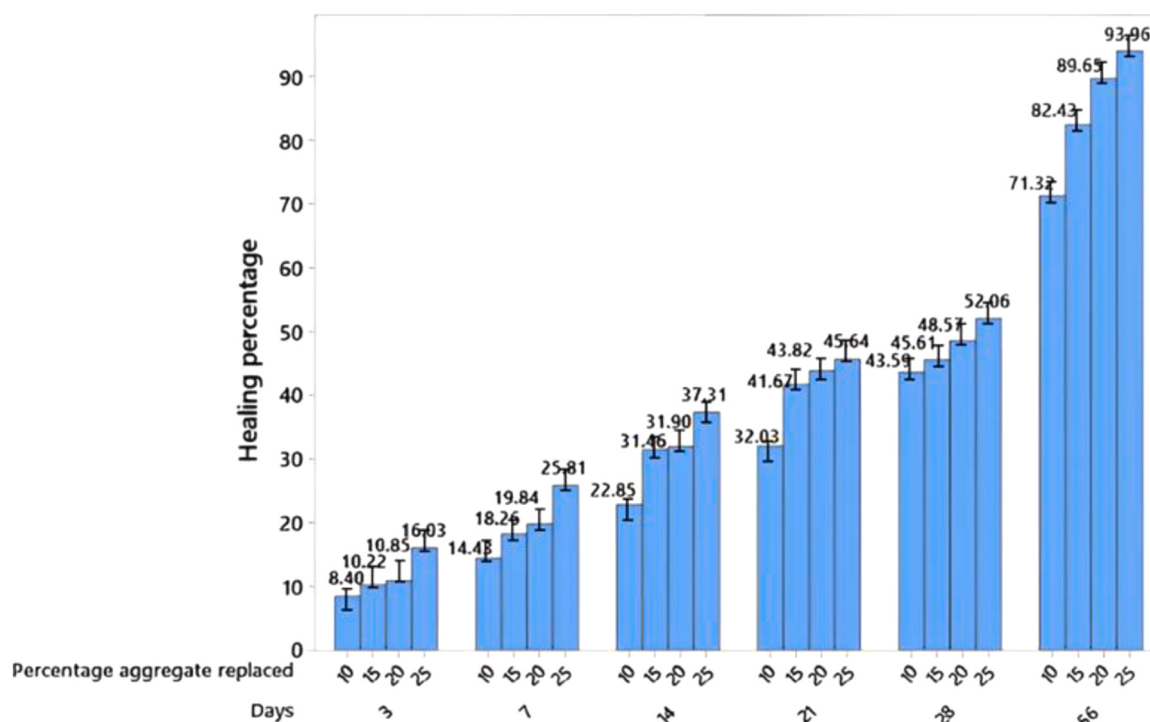


Fig. 13. Percentage healing of crack using UPV test.

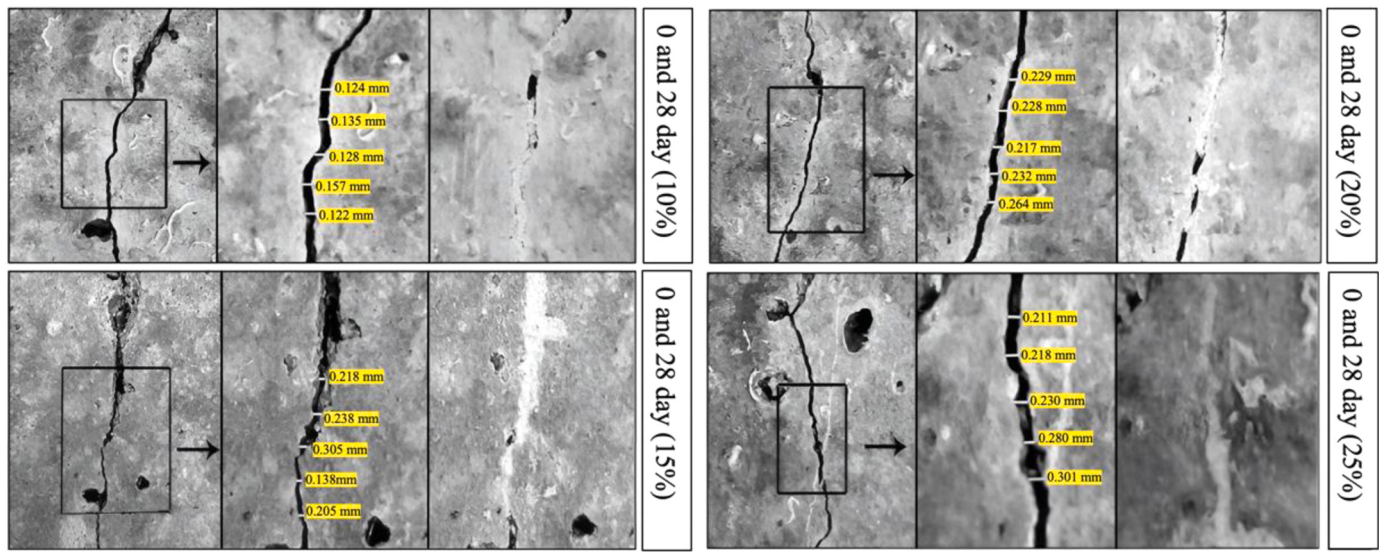


Fig. 14. Surface crack healing of specimen before and after 28 days.

**Table 4**

The average width of the specimen used for surface crack examination.

Specimen type	Average width (mm)
10%	0.133
15%	0.234
20%	0.219
25%	0.248

#### 4.6. Microstructural analysis of MICP and alginate

A small portion of the fragmented sample containing fractured CCAB of the healed specimen and the precipitate from the cracked area of the specimen were collected for examination using a field emission scanning electron microscope (FESEM). Energy dispersive X-ray spectroscopy (EDX) was used to analyse the precipitate's elements and morphological properties. Since the samples are non-conductive, the samples were gold coated before conducting FESEM analysis. For FESEM analysis, a coated

alginate bead which was collected from the broken sample of mortar was taken and observed as shown in Fig. 16(a). The bead observed was taken from the mortar matrix at a low magnification. A smooth surface texture of the bead can be observed. The outer layer of the bead was observed to be separated from the inner layer due to shear stresses developed during the application of load for breaking specimen. A sample collected from the crack location was observed and calcite precipitate was identified in crystalline form as shown in Fig. 16(b). The ettringite needles were also observed in samples collected from 56th day healed specimens as shown in Fig. 16(c). Bacillus megaterium cells were surrounded by  $\text{CaCO}_3$  precipitate and were found to be rod-shaped, as shown in Fig. 16(d). The cells were also completely struck inside the alginate layer of the bead. The sample shown in Fig. 16(b) was subjected to Energy Dispersive X-Ray analysis (EDX). The chemical composition and the scatter plot of calcium, carbon, and oxygen in the sample are shown in Fig. 17. The colour mapping for the same elements was also performed to visually identify the presence of chemical elements. From the observation it was found that calcium is present in abundance. It assists in the formation of end-product calcite, which eventually mends the crack.  $(\text{C}_6\text{H}_8\text{O}_6)_n$  is the

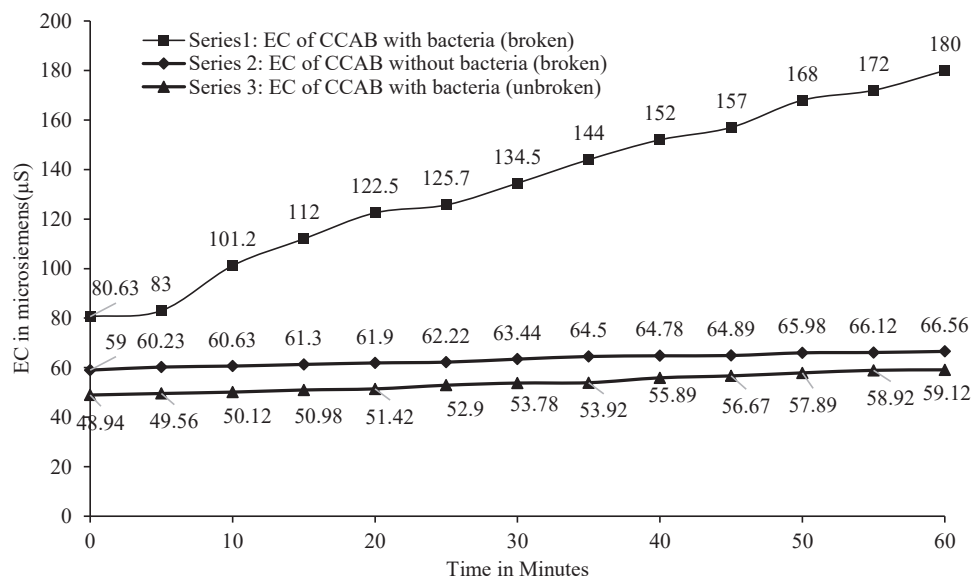
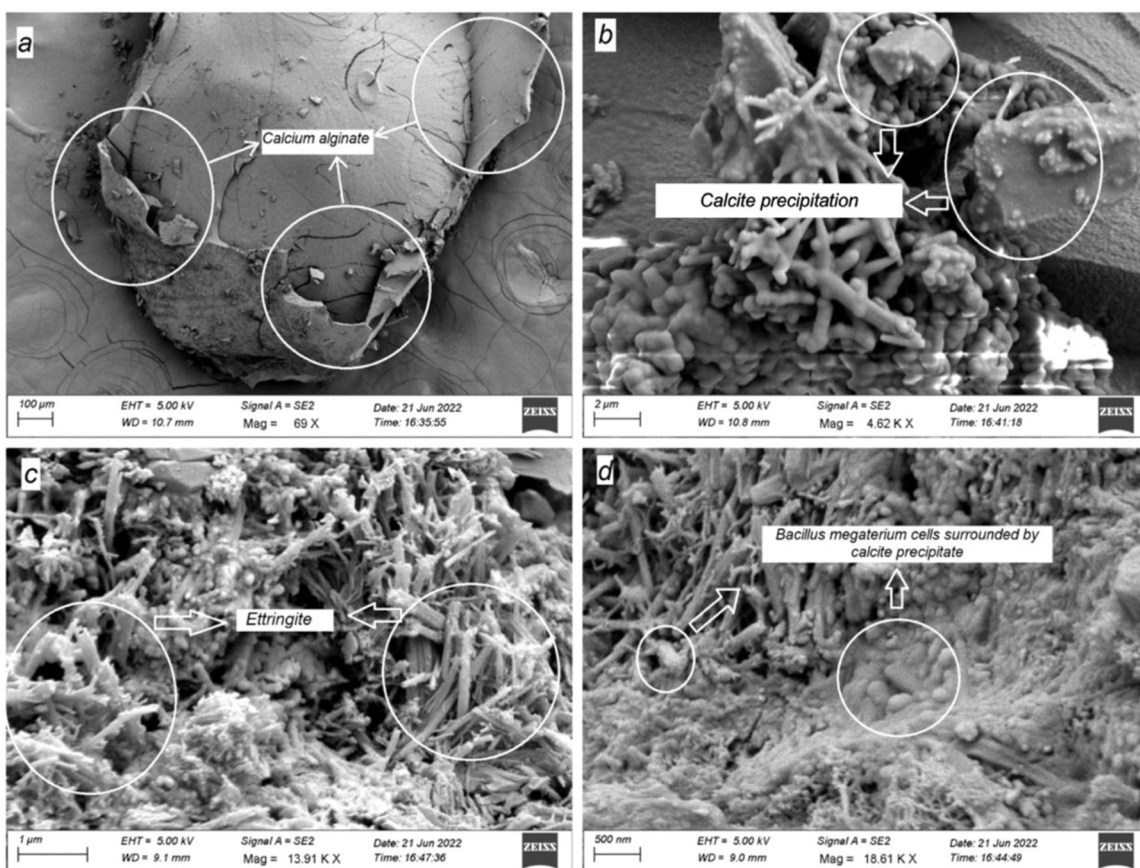


Fig. 15. Variation in electric conductivity.



**Fig. 16.** Calcite crystals at crack location, *Bacillus megaterium* in bead, and ettringite under FESEM: (a) Coated alginate bead; (b) Encapsulated bacterial cells in bead; (c) Ettringite needles in the mortar prepared with beads; (d) Bacteria cells and calcite precipitation at crack location.

structure of alginate polymer, calcium, and oxygen detected. Therefore, all the components in nutrient broth and alginate are detected in the sample. From Table 5, it can be seen that the weight percentages of the calcium, oxygen, carbon, sodium, and chlorine were 39.6%, 29.3%, 29.0%, 1.5%, and 0.6% respectively.

#### 4.7. Regression analysis

The test results were also subjected to regression analysis to generate the regression equation shown in Table 6. These regression equations can be used without experimentation to evaluate the related attributes within the tested ranges. Equation (10) shows the regression equation generated using Minitab software for the compressive strength and equation (11) and (12) can be used to find the percentage of healing. The prediction accuracy was based on the actual and predicted values.

#### 4.8. ANOVA analysis

The chosen model was statistically validated using analysis of variance (ANOVA), and the results for compressive strength, UPV test, and water permeability test are shown in Table 7.

The significance of the parameters impacting compressive strength (% aggregate replacement and nano-silica) and healing percentage was assessed using Minitab software (percentage aggregate replacement, days). Individual components were determined as significant variables based on a p-value less than 0.05 [32]. Every change in factors (variables) will significantly impact the reaction.

## 5. Conclusions and recommendations

The current study explored the performance of encapsulated bacteria-based self-healing cement mortar. The following conclusions can be drawn from the entire research work:

- The 10% CCAB and 5% nano-silica combination showed the maximum compressive strength (19.99 MPa). In specimens that included 25% CCAB and 5% nano-silica, compressive strength of 7.47 MPa was achieved. Since the strength falls short of the minimum criterion of 7.5 MPa outlined in IS 2250–1981, 25% replacement was discarded, even though this combination attains the highest healing. Although the maximum compressive strength achieved is 19.99 MPa with the 10% replacement, the 20% replacement can be considered ideal due to the strength of 11.64 MPa, which is sufficient.
- A maximum healing percentage of 83.30% was found in a 56-day water permeability test on the inside of the mortar for 20% aggregate replacement. The optimum healing rate for a 20% aggregate replacement after 56 days was reported to be 89.65% using the UPV test. Based on these, the best recovery occurs when 20% of FA is replaced with CCAB, which has a healing of at least 83.30% after 56 days.
- It may be deduced from above discussions that specimens with 20% FA replaced with CCAB and 5% NS added likewise satisfy the specifications for minimum compressive strength. So, 20% and 5% of CCAB and NS were considered as optimum.
- From the micro-structural studies based in FESEM and EDX analyses, it is evident from the shape of crystals and elemental analysis that the bacteria cells precipitate calcite around the cell walls.

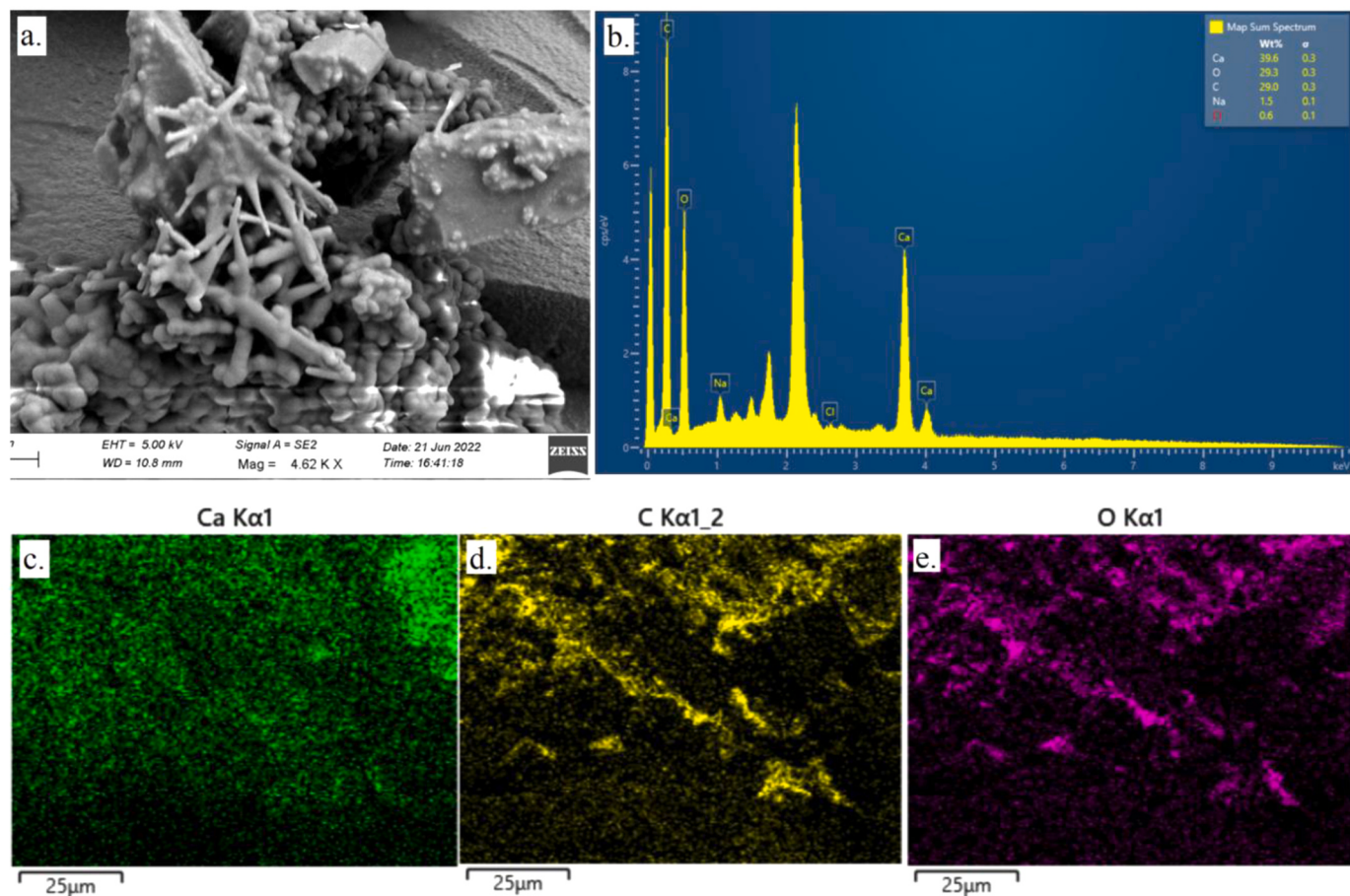


**Fig. 17.** Energy Dispersive X-Ray Analysis (EDX) results of calcite precipitation at crack location.

**Table 5**  
EDX analysis of calcite precipitation by *B. megaterium* at crack location.

Element	wt%	Atomic %
Ca K	39.6	50.00
O K	29.3	36.24
CK	29.0	12.79
Na K	1.5	0.91
Cl K	0.6	0.06
Total	100.00	100.00

**Table 6**  
Regression equations.

Test name	Regression equations	Prediction accuracy	Equation no.
Compressive test	$C = 24.2643 - 0.83465 A + 0.814464 B$ for B = 0–5% $C = 29.7327 - 0.804 A - 0.34375 B$ for B = 5–10%	96.20%	10
Water permeability	$P = -15.27 + 1.6263 A + 1.2246 D$	98.87%	11
UPV	$P = -4.34 + 0.832 A + 1.3423 D$	97.86%	12

where,  $A$  = percentage aggregate replacement,  $B$  = nano silica percentage,  $P$  = percentage of healing,  $C$  = compressive strength and  $D$  = days.

An average of 16.03% healing has been observed on the 3rd day in a 25% CCAB specimen, which is higher than all other percentages. This could be advantageous in the real-time scenario as it heals to a greater

amount quickly, preventing further crack propagation. Based on the study, it is also observed that various factors that may influence the amount of crack healing are the width of the crack, open/broken bacterial sources (CCAB in this study) along the undulated crack plane, percentage of the bacterial source added in any form, availability of moisture, availability of oxygen (if the bacteria is aerobic), and number of bacterial cells.

Further research can be done to investigate the variation of different parameters affecting the healing percentages to find the optimum amount of CCAB to be replaced with fine aggregate. Instead of adding *Bacillus megaterium* to the beads, other bacteria like *Bacillus sphaericus*, *Escherichia coli*, *Bacillus subtilis*, *Bacillus cohnii*, *Bacillus balodurans*, and *Bacillus pseudofirmus*, etc., can also be used. The performance of these micro-organisms in self-healing concrete has to be evaluated in further research. Although in this study, the decline in the compressive strength due to the addition of CCAB was compensated by adding nano-silica, further research concentrating on reducing the size of CCAB, which is 2.4 mm in the current investigation, may result in much higher strength without the addition of any more pozzolans.

#### CRediT authorship contribution statement

**Prabhath ranjan kumar soda:** Conceptualization, Methodology, validation, Investigation, Resources, Data curation, Writing - Original Draft. **Eluri kalyan Chakravarthy:** Software, Investigation, Formal analysis, Writing - Original draft. **Asheer mogal:** Software, Investigation, Formal analysis, writing - Original draft **Nikhil Thota:** software, investigation, Formal analysis. **Nimish bandaru:** investigation, Formal analysis. **Sanjay kumar Shukla:** Formal analysis, Writing - Review and Editing. **Mini K. M.:** Conceptualization, Methodology, Writing - Review

**Table 7**  
ANOVA analysis results.

Test name	Variables	Adj. sum of squares	Adj. mean Square	F-value	P-value	Significance
Compressive strength	Percentage Aggregate Replacement	1469.74	488.673	3692.12	0.00	Yes
	Nano Silica Percentage	38.41	14.96	95.002	0.00	Yes
Water Permeability	Percentage Aggregate Replacement	4073.02	1348.29	792.55	0.00	Yes
	Days	5211.49	1062.33	628.36	0.00	Yes
UPV	Percentage Aggregate Replacement	4642.786	1555.52	464.76	0.00	Yes
	Days	3538.75	873.909	259.89	0.00	Yes

and Editing, Supervision, Project administration.

### Declaration of Competing Interest

The authors declare that they have no known competing financial interests or personal relationships that could have appeared to influence the work reported in this paper.

### Data availability

Data will be made available on request.

### References

- [1] H. Singh, R. Gupta, Cellulose fiber as bacteria-carrier in mortar: Self-healing quantification using UPV, *J. Build. Eng.* 28 (2020), 101090, <https://doi.org/10.1016/j.jobe.2019.101090>.
- [2] R.M. Andrew, Global CO<sub>2</sub> emissions from cement production, *Earth Syst. Sci. Data* 10 (2018) 195–217, <https://doi.org/10.5194/essd-10-195-2018>.
- [3] S. Subash, V. Poornima, K. Jayanarayanan, A study on the effect of pH conditions on the properties of self-healing mortar cubes, in: IOP Conference Series: Materials Science and Engineering, Vol. 577, IOP Publishing., 2019, 012027.
- [4] H.A. Alqaifi, S.A. Bakar, A.R.Mohd Sam, A.R.Z. Abidin, S. Shahir, W.A.H. AL-Towayti, Numerical modeling for crack self-healing concrete by microbial calcium carbonate, *Constr. Build. Mater.* 189 (2018) 816–824, <https://doi.org/10.1016/j.conbuildmat.2018.08.218>.
- [5] Self-Healing Concrete and Cementitious Materials | IntechOpen, (n.d.). <https://www.intechopen.com/chapters/72141> (2022).
- [6] P. Ranjan, P. Soda, P. Venkatraman, R. Venkatasubramani, S. Venkataraman, Influence of ureolytic bacteria in improving performance characteristics of concrete, *Eco. Environ. Cons.* 23 (2017) 23.
- [7] J. Zhang, Y. Liu, T. Feng, M. Zhou, L. Zhao, A. Zhou, Z. Li, Immobilizing bacteria in expanded perlite for the crack self-healing in concrete, *Constr. Build. Mater.* 148 (2017) 610–617, <https://doi.org/10.1016/j.conbuildmat.2017.05.021>.
- [8] P.R.K. Soda, E.K. Chakravarthi, A. Mogal, K.M. Mini, Statistical and experimental investigation on self-healing of microcracks in cement mortar by encapsulation of calcite precipitating bacteria into expanded perlite, *Constr., Build. Mater.* 342 (2022), 127985, <https://doi.org/10.1016/j.conbuildmat.2022.127985>.
- [9] J.Y. Wang, N. De Belie, W. Verstraete, Diatomaceous earth as a protective vehicle for bacteria applied for self-healing concrete, *J. Ind. Microbiol. Biotechnol.* 39 (2012) 567–577, <https://doi.org/10.1007/s10295-011-1037-1>.
- [10] J. Xu, X. Wang, J. Zuo, X. Liu, Self-healing of concrete cracks by ceramics-loaded microorganisms, *Adv. Mater. Sci. Eng.* 2018 (2018) 1–8, <https://doi.org/10.1155/2018/5153041>.
- [11] W. Khaliq, M.B. Ehsan, Crack healing in concrete using various bio-influenced self-healing techniques, *Constr. Build. Mater.* 102 (2016) 349–357, <https://doi.org/10.1016/j.conbuildmat.2015.11.006>.
- [12] V. Sumithra, P.T. Ravichandran, K. D.K., Study on behaviour of self-healing concrete using silica gel, *Int. J. Eng. Technol.* 7 (2018) 411–414, <https://doi.org/10.14419/ijet.v7i2.12.11507>.
- [13] S. Han, E.K. Choi, W. Park, C. Yi, N. Chung, Effectiveness of expanded clay as a bacteria carrier for self-healing concrete, *Appl. Biol. Chem.* 62 (2019) 19, <https://doi.org/10.1186/s13765-019-0426-4>.
- [14] R. Alghamri, A. Kanellopoulos, A. Al-Tabbaa, Impregnation and encapsulation of lightweight aggregates for self-healing concrete, *Constr. Build. Mater.* 124 (2016) 910–921, <https://doi.org/10.1016/j.conbuildmat.2016.07.143>.
- [15] L. Jiang, G. Jia, C. Jiang, Z. Li, Sugar-coated expanded perlite as a bacterial carrier for crack-healing concrete applications, *Constr. Build. Mater.* 232 (2020), 117222, <https://doi.org/10.1016/j.conbuildmat.2019.117222>.
- [16] W. Dong, W. Li, K. Wang, S.P. Shah, D. Sheng, Multifunctional cementitious composites with integrated self-sensing and self-healing capacities using carbon black and slaked lime, *Ceram. Int.* 48 (14) (2022) 19851–19863.
- [17] W. Dong, W. Li, L. Shen, S. Zhang, K. Vessalas, Integrated self-sensing and self-healing cementitious composite with microencapsulation of nano-carbon black and slaked lime, *Mater. Lett.* 282 (2021), 128834.
- [18] J. Wang, A. Mignon, D. Snoeck, V. Wiktor, S. Van Vlierberghe, N. Boon, N. De Belie, Application of modified-alginate encapsulated carbonate producing bacteria in concrete: A promising strategy for crack self-healing, *Front. Microbiol.* 6 (2015) 1088.
- [19] M. Fahimizadeh, A. Diane Abeyratne, L.S. Mae, R.R. Singh, P. Pasbakhsh, Biological self-healing of cement paste and mortar by non-ureolytic bacteria encapsulated in alginate hydrogel capsules, *Materials* 13 (17) (2020) 3711.
- [20] Ross R.P. Fluorescens, and B. megaterium Effect on the lifespan of mutant-type dpy-11 and wild-type of *C. elegans*, *Cell Bio* 11 (1) (2022) 1–9.
- [21] N.K. Dhami, M.S.R. and A. Mukherjee, Biominerization of Calcium Carbonate Polymorphs by the Bacterial Strains Isolated from Calcareous Sites, 23, 2013: 707–714. <https://doi.org/10.4014/jmb.1212.11087>.
- [22] M.G. Giriselvam, V. Poornima, R. Venkatasubramani, V. Sreevidya, Enhancement of crack healing efficiency and performance of SAP in biocrete, in: IOP Conference Series: Materials Science and Engineering, Vol. 310, IOP Publishing., 2018, 012061.
- [23] P.R.K. Soda, M. M.K., Performance enhancement and remediation of microcracks in cement mortar by doping calcite-precipitating microorganisms, *J. Mater. Civ. Eng.* 34 (2022) 04022035, [https://doi.org/10.1061/\(ASCE\)MT.1943-5533.0004176](https://doi.org/10.1061/(ASCE)MT.1943-5533.0004176).
- [24] A. Ranga Rao, V. Baskaran, R. Sarada, G.A. Ravishankar, In vivo bioavailability and antioxidant activity of carotenoids from microalgal biomass — A repeated dose study, *Food Res. Int.* 54 (2013) 711–717, <https://doi.org/10.1016/j.foodres.2013.07.067>.
- [25] M.W. Ullah, W.A. Khattak, M. Ul-Islam, S. Khan, J.K. Park, Encapsulated yeast cell-free system: A strategy for cost-effective and sustainable production of bio-ethanol in consecutive batches, *Biotechnol. Bioproc E* 20 (2015) 561–575, <https://doi.org/10.1007/s12257-014-0855-1>.
- [26] IS 4031–6 (1988): Methods of physical tests for hydraulic cement, Part 6: Determination of compressive strength of hydraulic cement (other than masonry cement), (n.d.) 11.
- [27] IS 12269 (1987): 53 grade ordinary Portland cement, (n.d.) 17.
- [28] V. Poornima, R. Venkatasubramani, V. Sreevidya, S. Subash, J. Karingamanna, Environmental influence on bacterial efficiency in ensuring self-healing mortars, *Eur. J. Environ. Civ. Eng.* (2021).
- [29] IS 3085 (1965): Method of Test for Permeability of Cement Mortar and Concrete, (n.d.) 15.
- [30] S.C. Chuo, S.F. Mohamed, S.H. Mohd Setapar, A. Ahmad, M. Jawaid, W.A. Wani, A. A. Yaqoob, M.N. Mohamad Ibrahim, Insights into the current trends in the utilization of bacteria for microbially induced calcium carbonate precipitation, *Mater. (Basel)* 13 (2020), E4993, <https://doi.org/10.3390/ma13214993>.
- [31] D. Kong, Y. Su, X. Du, Y. Yang, S. Wei, S.P. Shah, Influence of nano-silica agglomeration on fresh properties of cement pastes, *Constr. Build. Mater.* 43 (2013) 557–562, <https://doi.org/10.1016/j.conbuildmat.2013.02.066>.
- [32] P.R. Kumar Soda, K. Chakravarthi, K.M. Mini, Experimental and statistical investigation on strength and microcracks remediation in cement mortar using expanded vermiculite as a bacterial carrier, *J. Build. Eng.* 63 (2022), 105567, <https://doi.org/10.1016/j.jobe.2022.105567>.
- [33] Mohammad Khaneghahi, Divya Kamireddi, Seyed Ali Rahmaninezhad, Caroline Schauer, Christopher Sales, Ahmad Najafi, Aidan Cotton, Amir Sadighi, Yaghoob Farnam, Development of bio-inspired multi-functional polymeric-based fibers (BioFiber) for advanced delivery of bacterial-based self-healing agent in concrete, in: MATEC Web of Conferences, Vol. 378, EDP Sciences,, 2023, p. 02001, <https://doi.org/10.1051/matecconf/202337802001>.